

## Runaway Electrification of Friable Self-Replicating Granular Matter

Julyan H. E. Cartwright,<sup>\*,†</sup> Bruno Escrivano,<sup>\*,‡</sup> Hinrich Grothe,<sup>\*,§</sup> Oreste Piro,<sup>\*,||</sup>  
C. Ignacio Sainz Díaz,<sup>\*,†</sup> and Idan Tuval<sup>\*,⊥</sup>

<sup>†</sup>Instituto Andaluz de Ciencias de la Tierra (IACT), CSIC–Universidad de Granada, E-18100 Armilla, Granada, Spain

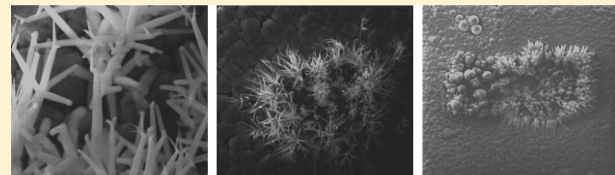
<sup>‡</sup>Basque Center for Applied Mathematics (BCAM), Alameda de Mazarredo 14, E-48009 Bilbao, Basque Country, Spain

<sup>§</sup>Institut für Materialchemie, Technische Universität Wien, Getreidemarkt 9/BC/01, A-1060 Vienna, Austria

<sup>||</sup>Departament de Física, Universitat de les Illes Balears, E-07122 Palma de Mallorca, Spain

<sup>⊥</sup>Institut Mediterrani d'Estudis Avanats (IMEDEA), CSIC–Universitat de les Illes Balears, E-07190 Mallorca, Spain

**ABSTRACT:** We establish that the nonlinear dynamics of collisions between particles favors the charging of an insulating, friable, self-replicating granular material that undergoes nucleation, growth, and fission processes; we demonstrate with a minimal dynamical model that secondary nucleation produces a positive feedback in an electrification mechanism that leads to runaway charging. We discuss ice as an example of such a self-replicating granular material: We confirm with laboratory experiments in which we grow ice from the vapor phase *in situ* within an environmental scanning electron microscope that charging causes fast-growing and easily breakable palmlike structures to form, which when broken off may form secondary nuclei. We propose that thunderstorms, both terrestrial and on other planets, and lightning in the solar nebula are instances of such runaway charging arising from this nonlinear dynamics in self-replicating granular matter.



### INTRODUCTION

Charging of grains of identical insulating materials during collisions has been of considerable interest recently, both for its intrinsic physics and for its applications to situations ranging from volcanic dust plumes and desert sandstorms to industrial powder processing.<sup>1,2</sup> However, work up to now has not explained why in some instances charging grows, rather than diminishes as one might naively expect, and can run away extremely rapidly, leading to electrical discharges: lightning. Outstanding examples of runaway collisional charging involve ice, in thunderstorms both on Earth<sup>3</sup> and on other planets,<sup>4,5</sup> and, it is speculated, in the solar nebula;<sup>6–8</sup> these instances concern granular media whose particles also undergo nucleation, growth, and fission, so that they, in effect, reproduce. In this work, we demonstrate with a minimal dynamical model that secondary nucleation, production of a new particle from an existing particle, is a key process in producing runaway electrical charging in self-replicating granular matter. We concomitantly present the results of experiments on growing ice *in situ* from the vapor phase within an environmental scanning electron microscope. We show that an effect of the electric field is to induce the formation of fast-growing ice “palms” intermediate in morphology between whiskers and dendrites; the ease of breakage of these palmlike formations will clearly favor secondary nucleation and hence runaway electrification.

“In a thousand seconds, more or less, its volume increases a thousandfold, the intensity of its electric fields increases a thousandfold, and its electric energy increases a billionfold”; thus described Vonnegut the tremendous metamorphosis a

cumulus cloud undergoes to become a cumulonimbus or thundercloud.<sup>3</sup> Thundercloud electrification is a consequence of ice particles colliding within a cloud and exchanging electrical charge. Charge dipole development in a thunderstorm is due to the physical separation of particles with opposite charges inside the cloud: Larger, heavier particles will fall, while smaller, lighter particles will rise in the updraft, owing to their different dynamics,<sup>9</sup> and these particles carry different charges.<sup>10</sup> Usually, in thunderstorms, the smaller ice particle is an ice crystal and carries positive charge aloft in the updraft; the larger graupel ice particle falls with an opposite negative charge, leading to a typical thunderstorm. We may contrast the foregoing with charging in other granular media,<sup>11,12</sup> where it has been argued that simple geometry, without growth and fission processes, leads to a net transfer of electrons from larger to smaller particles,<sup>1</sup> so that smaller particles tend to charge negatively and larger ones positively. Whether this differential charging tendency operates one way or the other depends on the microphysics, which differs for different materials, so this polarity differs. For our present purposes, however, what is relevant is that there should exist such a triboelectric charging tendency in one sense or the other. Here we build a minimal model (Figure 1) incorporating solely the collisional dynamics of charge transfer plus nucleation, growth, and fission processes, which we aim to have general relevance to self-replicating granular media.

**Received:** July 8, 2013

**Revised:** September 2, 2013

**Published:** September 16, 2013

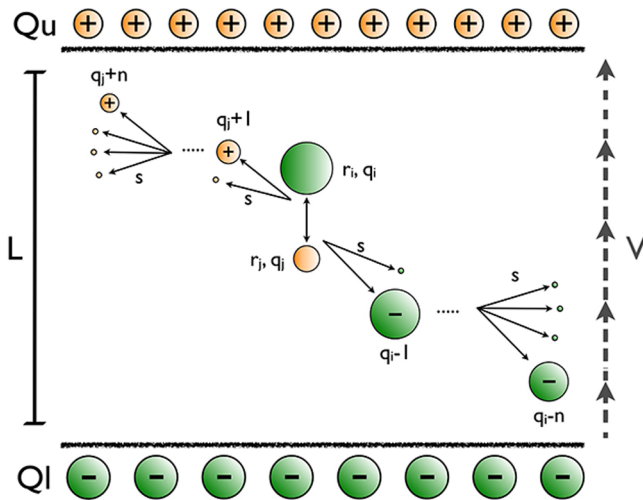


**Figure 1.** Anatomy of our minimal model of charging of friable self-replicating granular matter through secondary nucleation, incorporating the processes of particle growth ( $r_i \rightarrow r_i + 1$ ), advection (with speed  $u_i$ ), collision, charge transfer, and fission (with probability  $s$ ).

## CHARGING MODEL

We consider (Figure 1) a one-dimensional system of length  $L$ , within which we place randomly  $n$  neutrally charged particles,  $q_i = 0$  for  $i = 1, \dots, n$ , of size  $r_i$  extracted from a Gaussian distribution of sizes with mean  $\bar{r} = 1$  and standard deviation  $\sigma$ . These particles grow at a constant rate, independent of particle size, that sets the time scale of the problem. At the same time, they sediment in an upward flow of constant magnitude at their terminal velocity,  $u_i$ , determined by the instantaneous balance of fluid drag and gravitational forces. The sedimentation speed is normalized by the updraft speed (i.e.,  $u_i = 1$  for passive tracers) and is approximated by a linear function of the particle size  $r_i$ ,  $u_i = 1 - (r_i/R_c)$ . This function is positive (negative) for  $r_i$  below (above) a critical value  $R_c$ . The sedimentation speed of all particles in the simulation is updated every integration time step; in this way, small particles that are initially advected upward by the updraft slow their upward motion as they grow and begin moving downward after reaching the threshold  $R_c$ .

When the trajectories of two particles  $i$  and  $j$  cross, they collide. To overcome the 1D limitation of the model, we allow particles to get past one another after the collision, so that after each time step particles end up in whatever final position their velocities prescribe. Both mass and charge are conserved during a collision but, while charge is transferred in every collision (the smaller particle leaving the collision positively charged:  $q_i \rightarrow q_i + 1$  and  $q_j \rightarrow q_j - 1$  with  $r_i < r_j$ ), mass is only transferred if fission occurs through secondary nucleation. We assign a certain probability  $s$  for fission to occur for each of the two particles involved in a collision. If fission does occur for particle  $i$ , a new, neutrally charged particle with radius 1 splits from it, reducing its size to  $r_i = r_i - 1$ . Although fracture of particles has been shown to lead to additional charging,<sup>13</sup> we left this effect out of the model for the sake of simplicity as it does not change qualitatively the presented results.

Boundary conditions are absorbing: particles leaving the system through the upper or lower boundary are absorbed there, and do not participate further in the dynamics, but their charge accumulates to the total charge at the boundaries:  $Q_{u(l)} = \sum q_i$  for  $i$  leaving the system through the upper (lower)

boundary, respectively. The total large-scale charge separation is calculated as  $\Delta Q = Q_u - Q_l$ .

For given initial conditions (set completely by the concentration of particles,  $\rho = n/L$ , and the initial spread of the size distribution,  $\sigma$ ), the behavior of our minimal model then depends on just two parameters, the critical radius  $R_c$  and the secondary nucleation rate  $s$ . In what follows, we set  $R_c = 8$ ,  $\rho = 2$  and  $\sigma = 0.1$  and explore the behavior of the model with respect to the secondary nucleation rate  $s$ . We note that electric forces are not considered in the model but implicitly (through the secondary nucleation rate responsible for the process of fission).

Figure 2 displays the typical transient dynamics of the charge distribution in the model. Charge separation events at two

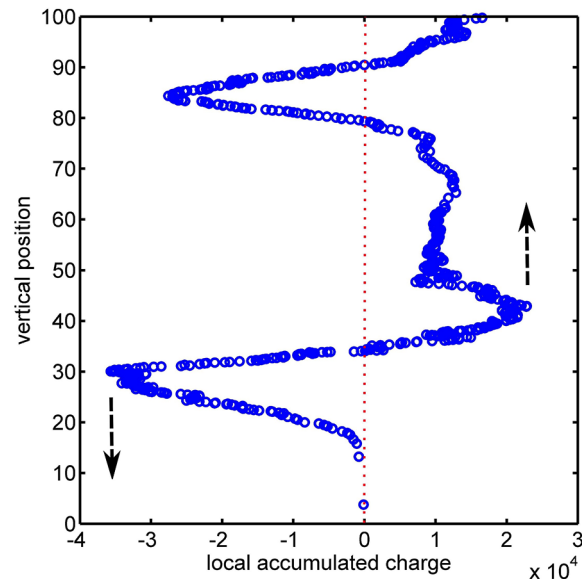


**Figure 2.** Typical transient charge distribution in the model at  $t = 30$ . Charge separation events at two positions are clearly visible. As time passes, light positively charged particles move toward the upper boundary while heavy negatively charged ones move in the opposite direction, as indicated by arrows, contributing to a non-negligible large-scale dipolar charge distribution  $\Delta Q$ . The neutral charge line (dotted) is marked for reference.

vertical positions are clearly visible. The figure shows an initial stage in the transient dynamics chosen to exemplify how the charge separation process operates in the model. As time passes, as indicated by black arrows, light positively charged particles move toward the upper boundary while heavy negatively charged ones move in the opposite direction, contributing to a non-negligible dipolar large scale charge separation  $\Delta Q$ . Regions where localized collisions are produced generate large charges that are then separated by differential advection. Even at those early stages in the process, the global dipolar structure of the system, quantified by the large-scale charge difference between the boundaries  $\Delta Q$ , is the dominant field. Figure 3 shows particle size and charge distributions for the upper and lower boundaries. Charge separation correlated with particle size separation is observed.

We display the dynamics of the total charge separation  $\Delta Q$  in Figure 4. The total charge separation  $\Delta Q$  at a finite time step (which is a measure of the speed of the charge-separation process) displays nonmonotonic discontinuous behavior as a function of the secondary nucleation rate  $s$ . Below a critical

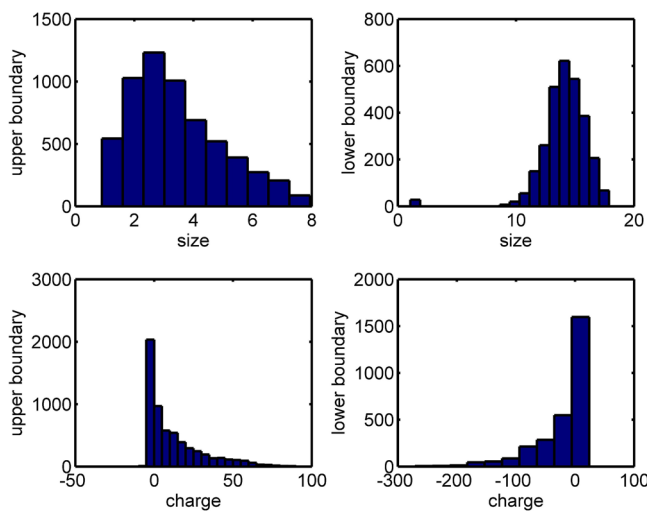


**Figure 3.** Particle size ( $r_j$ ) and charge ( $q_j$ ) distributions for the system upper boundary (left panels) and lower boundary (right panels). Charge separation, correlated with particle size separation, is observed.

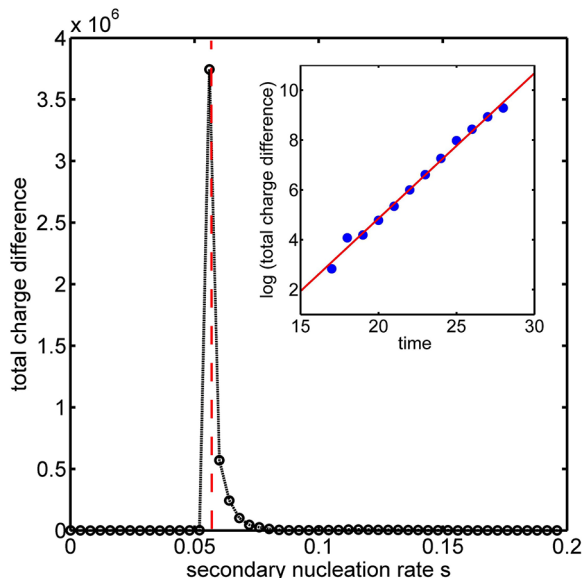


**Figure 4.** Charge separation shown at a finite time step in the simulation. The total charge separation  $\Delta Q$  displays nonmonotonic behavior as a function of the secondary nucleation rate  $s$ . Inset: time evolution of  $\Delta Q$  for  $s = 0.1$  shows the exponential growth characteristic of all values of  $s > s_c$ .

value  $s_c$ , the long-term dynamics reaches an emptying state with no particles left in the domain and a finite (and small) final charge separation; as there are few secondary nuclei, the initial particles grow and collide very little before leaving the system. Occasionally some charge is produced, but not much. Above  $s_c$ , the number of collisions grows, and with it the charge transfer. As the charge acquired by the particles is correlated with their size, charge separation occurs too. The system approaches a steady state with an average nonzero number of particles in the domain and an exponentially divergent charge separation, as shown in the inset of Figure 4. This exponential charge growth is limited in nature by electrical discharges, "lightning".

However, for secondary-nucleation rates much greater than  $s_c$ , there are more and more collisions. The particles undergo more fission into secondary nuclei, and although much charge

is produced, it does not separate as well; charge separation is still exponentially divergent, but the growth rate decreases beyond  $s_c$ . There is thus an intermediate optimal value of the secondary nucleation rate to produce the greatest charge separation. This critical value  $s_c \approx 1/(\rho R_c)$  is 0.0625 in the simulations (dashed line in Figure 4). A smaller value of  $R_c$  (which means a weaker updraft) requires secondary nucleation to occur more often (larger  $s_c$ ) in order to ensure some particles are advected upward (leading to charge separation), while the initial density of particles,  $\rho$ , controls the collision probability. It is worth mentioning that even in the limit of very high particle density  $\rho$ , in which many collisions occur at early stages, charge separation is minimal in the absence of secondary nucleation. It is the latter that is responsible for the observed discontinuous critical behavior.

## ■ LABORATORY EXPERIMENTS

Earlier work of ours made us suspect that secondary nucleation ought to be important in runaway collisional charging. Previously we have shown that the nonlinear feedback effects of secondary nucleation are responsible for chiral symmetry breaking in experiments involving crystallizing a chiral chemical compound from solution.<sup>14,15</sup> We showed that secondary nuclei in such stirred crystallization experiments are often easily detached whisker or needle crystallites growing from a mother crystal, and a runaway process involving the formation of secondary nuclei leads to complete chiral symmetry breaking.

Water molecules possess a high electric polarizability; they are electrical dipoles and can be highly affected by the presence of an external field. During dendrite growth, an electric field can produce an ordering of the molecular dipoles and increase the molecular flow toward the dendrite tip. This increases the growth velocity, decreases the tip radius and disables the generation of side-branches, producing long whiskers. These effects have long been noted<sup>10</sup> and were studied quantitatively by Libbrecht and Tanusheva,<sup>16</sup> who measured the tip velocity and found that high voltages could multiply the growth rate more than 10-fold.

We hypothesized that this dendrite growth mechanism should be involved in promoting secondary nucleation. Thus, we undertook laboratory experiments to see whether similarly easily detached forms as in solution crystallization experiments are produced in ice under the influence of an electric field. We employed a FEI Quanta 200 environmental scanning electron microscope (ESEM) equipped with a liquid nitrogen cold stage to grow ice in situ at low pressures and at temperatures of 90–200 K. The microscope was set up so that the cold finger, together with a thermostat, was directly beneath the substrate (a silicon wafer attached with silver glue). We began by evacuating the chamber in the high-vacuum mode of the microscope ( $6 \times 10^{-4}$  Pa) and lowering the substrate to the working temperature. We first scanned the uncovered sample substrate, on which we grew an ice film by switching to low-vacuum mode and opening the water input microvalve at a pressure of 40 Pa for some seconds. We found this was the highest pressure at which we could obtain clear images. We closed the microvalve at or before the point when the substrate temperature increases and cannot be maintained at the working temperature, following which we switched back to high-vacuum mode and observed the ice growth in situ.

In the electron-microscope chamber, a high-voltage electron beam is used for imaging, and as we display in Figure 5, we find that the electric field produces rapid dendrite growth wherever

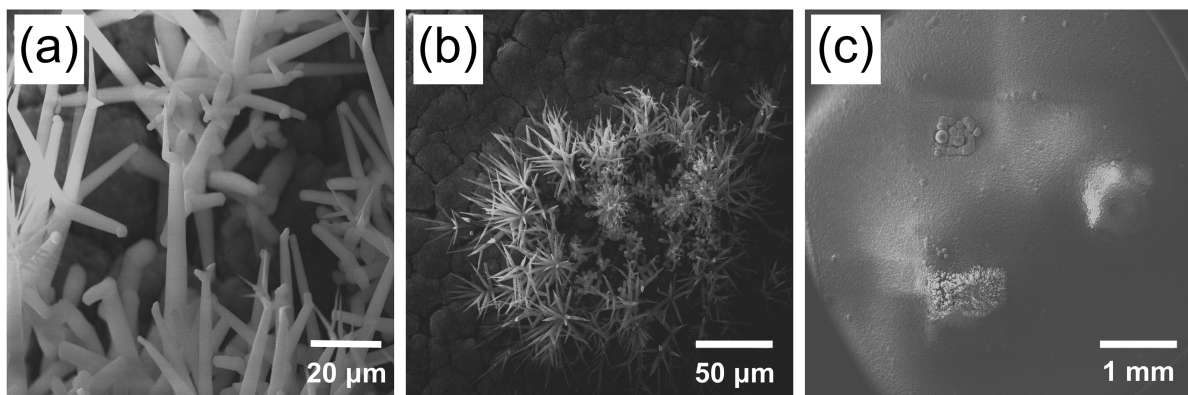


**Figure 5.** An electric field promotes ice “palm” growth in an ESEM: (a, b) At  $T = 170$  K,  $P = 40$  Pa,  $V = 30$  kV, an ice “forest” is rapidly formed. The forest displays the morphology intermediate between whiskers and dendrites typically formed with charged ice. (c) In an overview, the three zones where we imaged and charged with electrons stand out, showing the increased growth on the background ice film.

we charge with electrons by imaging. A typical ice morphology seen under these circumstances is of a form intermediate between whiskers and dendrites, which often takes on the aspect of a palm tree; see Figure 5a. As we zoom out (Figure 5b, c), we note that the palm forest is found only where we had been imaging; outside the area of the electron beam, we find a relatively flat film of ice, while within the imaged zones, three in Figure 5c, we find faster ice growth and the ice forest.

We had noted such palmlike forms in previous experiments involving growing ice inside an electron microscope,<sup>17</sup> but had not then realized that the electric field was involved in their production. These experiments are necessarily qualitative, being performed within the chamber of an unmodified ESEM, but we find the results suggestive: Owing to their geometry, the breakage of these structures on collision is likely and will lead to the formation of new nucleation centers. Such friable morphologies do not only form in ice under electric fields; snowflakes too have such delicate structures, but an electric field promotes this form of growth.<sup>16</sup>

## CONCLUSIONS

Our minimal physical model of a self-replicating granular material shows how secondary nuclei from such growth can lead to runaway charging. These effects may be present in ice on Earth, in terrestrial thunderstorms,<sup>3</sup> and in astrophysical ices, in the solar nebula,<sup>6–8</sup> and in thunderstorms on other planets,<sup>4,5</sup> some of which, for example, on Venus, may involve self-replicating granular materials other than water ice. It is conceivable that this dynamics is involved in the formation of the Martian geological structures called razorbacks.<sup>18</sup> While ice<sup>19</sup> is clearly the most quotidian example of a friable self-replicating granular material, one that breaks easily and continues to grow, other such materials can be both sought in different astrophysical environments, and also produced in technological contexts.

## AUTHOR INFORMATION

### Corresponding Authors

- \*E-mail: julyan.cartwright@csic.es.
- \*E-mail: bescribano@bcamath.org.
- \*E-mail: hgrothe@tuwien.ac.at.
- \*E-mail: piro@imedea.uib-csic.es.
- \*E-mail: ignacio.sainz@iact.ugr-csic.es.
- \*E-mail: ituval@imedea.uib-csic.es.

### Notes

The authors declare no competing financial interest.

### ACKNOWLEDGMENTS

We thank Werner Kuhs and Emmanuel Villermaux for useful discussions and Karin Whitmore for her assistance in the electron microscopy sessions. We acknowledge the financial support of the Spanish MICINN Grant FIS2010-22322-C01 (O.P. and I.T.), “subprograma Ramón y Cajal” (I.T.), and grant FIS2010-22322-C02 (J.H.E.C. and C.I.S.D.); and the Austrian Science Fund (FWF), Grant P23027 (H.G.). All the authors contributed substantially to this work; the author ordering is alphabetical.

### REFERENCES

- (1) Kok, J. F.; Lacks, D. J. Electrification of granular systems of identical insulators. *Phys. Rev. E* **2009**, *79*, 051304.
- (2) Pähzt, T.; Herrmann, H. J.; Shinbrot, T. Why do particle clouds generate electric charges? *Nat. Phys.* **2010**, *6*, 364–368.
- (3) Vonnegut, B. The atmospheric electricity paradigm. *Bull. Am. Meteorol. Soc.* **1994**, *75*, 53–61.
- (4) Aplin, K. L. Atmospheric electrification in the solar system. *Surv. Geophys.* **2006**, *27*, 63–108.
- (5) Yair, Y. Charge generation and separation processes. *Space Sci. Rev.* **2008**, *137*, 119–131.
- (6) Gibbard, S. G.; Levy, E. H. On the possibility of lightning in the protosolar nebula. *Icarus* **1997**, *130*, 517–533.
- (7) Pilipp, W.; Hartquist, T. W.; Morfill, G. E.; Levy, E. Chondrule formation by lightning in the protosolar nebula? *Astron. Astrophys.* **1998**, *331*, 121–146.
- (8) Muranushi, T. Dust–dust collisional charging and lightning in protoplanetary discs. *Mon. Not. R. Astron. Soc.* **2010**, *401*, 2641–2664.
- (9) Cartwright, J. H. E.; Feudel, U.; Károlyi, G.; de Moura, A.; Piro, O.; Tél, T. Dynamics of finite-size particles in chaotic fluid flows. In *Nonlinear Dynamics and Chaos: Advances and Perspectives*; Thiel, M., Kurths, J., Romano, M. C., Károlyi, G., Moura, A., Eds.; Springer: Berlin, 2010.
- (10) Mason, B. J. *The Physics of Clouds*; Oxford University Press: Oxford, U.K., 1971.
- (11) Shinbrot, T.; Komatsu, T. S.; Zhao, Q. Spontaneous tribocharging of similar materials. *Europhys. Lett.* **2008**, *83*, 24004.
- (12) Lacks, D. J.; Sankaran, R. M. Contact electrification of insulating materials. *J. Phys. D* **2011**, *44*, 453001.
- (13) Avila, E. E.; Caranti, G. M. A laboratory study of static charging by fracture in ice growing by riming. *J. Geophys. Res.: Atmos.* **1994**, *99*, 10611–10620.
- (14) Cartwright, J. H. E.; García-Ruiz, J. M.; Piro, O.; Sainz-Díaz, C. I.; Tuval, I. Chiral symmetry breaking during crystallization: an

advection-mediated nonlinear autocatalytic process. *Phys. Rev. Lett.* **2004**, *93*, 035502.

(15) Cartwright, J. H. E.; Piro, O.; Tuval, I. Ostwald ripening, chiral crystallization, and the common-ancestor effect. *Phys. Rev. Lett.* **2007**, *98*, 165501.

(16) Libbrecht, K. G.; Tanusheva, V. M. Electrically induced morphological instabilities in free dendrite growth. *Phys. Rev. Lett.* **1998**, *81*, 176.

(17) Cartwright, J. H. E.; Escribano, B.; Sainz-Díaz, C. I. The mesoscale morphologies of ice films: porous and biomorphic forms of ice under astrophysical conditions. *Astrophys. J.* **2008**, *687*, 1406–1414.

(18) Shinbrot, T.; LaMarche, K.; Glasser, B. Triboelectrification and razorbacks: geophysical patterns produced in dry grains. *Phys. Rev. Lett.* **2006**, *96*, 178002.

(19) Bartels-Rausch, T.; Bergeron, V.; Cartwright, J. H. E.; Escribano, R.; Finney, J. L.; Grothe, H.; Gutierrez, P. J.; Haapala, J.; Pettersson, J. B. C.; Price, S. D.; Sainz-Diaz, C. I.; Stokes, D. J.; Strazzulla, G.; Thomson, E. S.; Trinks, H.; Uras-Aytemiz, N. Ice structures, patterns, and processes: a view across the icefields. *Rev. Mod. Phys.* **2012**, *84*, 885–944.